Available online at www.sciencedirect.com

ScienceDirect

journal homepage: www.elsevier.com/locate/he

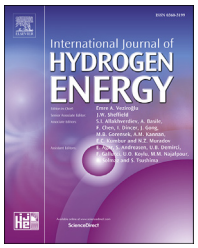

Modeling hydrogen storage on Mg–H_2 and $LiNH_2$ under variable temperature using multiple regression analysis with respect to ANOVA

Farqad Al-Hadeethi [a,*], *Naseem Haddad* [a], *Adi Said* [a], *Hatem Alsyouri* [b,c], *Amani Abdelhadi* [a]

[a] *Research and Development, Royal Scientific Society, Amman, Jordan*
[b] *Department of Chemical Engineering, School of Engineering, The University of Jordan, Amman, Jordan*
[c] *Department of Chemical Engineering, College of Engineering and Technology, American University of the Middle East, Egaila, Kuwait*

ARTICLE INFO

Article history:
Received 17 December 2016
Received in revised form
26 April 2017
Accepted 13 May 2017
Available online 12 June 2017

Keywords:
Hydrogen
Storage
Metal hydrides
Modelling

ABSTRACT

The world is facing a major problem due to the depletion of conventional energy sources. Hydrogen is considered one of the most promising sources of energy. Recently, one of the problems facing utilization of hydrogen energy is the storage. Therefore, finding materials to store hydrogen based on the adsorption/desorption methodology (i.e. metal hydrides) is considered extremely vital issue. During this work two candidate materials (i.e. Mg–H_2 and $LiNH_2$) were investigated at different temperatures (25–45 °C). The results revealed that both candidate materials possessed long cycle life and cyclibility which opens the wide door to use these materials in vehicular applications. On the other hand the generated mathematical models based on the multiple regression analysis with respect to ANOVA showed that increasing temperature will increase the weight of hydrogen adsorption for both candidate materials.

Introduction

Hydrogen fuel is an attractive alternative source of energy since it is clean, non-toxic and renewable especially when it is produced from renewable resources (i.e. Sea Water and Solar Energy) [1], making it as a substitute for petroleum derived fuels in vehicular applications. However, the greatest challenge in making hydrogen available for use in transportation lies in the development of safe, compact, portable and cost effective hydrogen storage systems. Hydrogen can be stored as (i) pressurized gas, (ii) cryogenic liquid, (iii) solid fuel as chemical or physical combination with materials, such as metal hydrides and Metal Organic Frameworks (MOFs). Metal hydrides compose of metal atoms that constitute a host lattice and hydrogen atoms. Hydrogen storage in metal hydrides depends on different parameters and consists of several mechanistic steps. Metals differ in the ability to dissociate hydrogen, this ability being dependent on:

* *Corresponding author.*
E-mail address: farqad.hadeethi@rss.jo (F. Al-Hadeethi).
http://dx.doi.org/10.1016/j.ijhydene.2017.05.101

A. Surface structure.
B. Morphology and purity.

An optimum hydrogen-storage material is required to have the following properties [2,3]:

A. High hydrogen capacity per unit mass and unit volume which determines the amount of available energy.
B. Low dissociation temperature.
C. Moderate dissociation pressure.
D. Low heat of formation in order to minimize the energy necessary for hydrogen release.
E. Low heat dissipation during the exothermic hydride formation.
F. Reversibility.
G. Limited energy loss during charge and discharge of hydrogen.
H. Fast kinetics.
I. High stability against O_2 and moisture for long cycle life.
J. Cyclibility.
K. Low cost of recycling and charging infrastructures.
L. High safety.

There is considerable research on magnesium and its alloys due to their high hydrogen storage capacity by weight and low cost. Besides, the Mg-based hydrides possess good-quality functional properties, such as heat-resistance, vibration absorbing, reversibility and recyclability. Several researchers have investigated magnesium and its alloys from various angles. Fry et al. [4] have improved hydrogen cycling kinetics of nano-structured magnesium/transition metal multilayer thin films, while Shahi et al. [5] have conducted studies on de/rehydrogenation characteristics of nanocrystalline Mg–H_2 co-catalysed with Ti, Fe and Ni. James Jr. et al. [6] have studied the fundamental environmental reactivity testing and analysis of the hydrogen storage material $2LiBH_4{\cdot}MgH_2$. Utke et al. [7] have investigated the effect of using $2LiBH_4$–MgH_2 for reversible hydrogen storages. Mustafa et al. [8] have studied the influence of adding K_2TiF_6 on the hydrogen sorption properties of MgH_2. Song et al. [9] have investigated the improvement of hydrogen-storage properties of MgH_2 by adding Ni, $LiBH_4$, and Ti. Gattia et al. [10] have studied the effect of hydrogen cycling on the microstructure and morphological changes in MgH_2. Korablov et al. [11] have investigated activation effects during hydrogen release and uptake from MgH_2. It is worth of mention that Shao et al. [12] have studied the hydrogen storage and thermal conductivity of Mg–based materials while Rusman et al. [13] have conducted a review on the current progress of metal hydrides for solid-state hydrogen storage applications. Tran et al. [14] have investigated the dehydriding mechanism of Mg_2NiH_4 using in-situ ultra-high voltage transmission electron microscopy (TEM) combined with Synchrotron powder X-ray diffraction (XRPD) and differential scanning calorimetry (DSC).They found that the hydrogen release is based on a mechanism of nucleation and growth of Mg_2NiHx ($x \sim 0$–0.3) solid solution grains which is greatly enhanced in the presence of crystal defects occurring as a result of the polymorphic phase transformation. Li et al. [15] investigated the hydrogen storage properties and mechanisms of the Ca $(BH_4)_2$-added $2LiNH_2$–MgH_2 system. The results indicated that the dehydrogenated $2LiNH_2$–MgH_2–0.1Ca $(BH_4)_2$ sample could absorb 4.7 wt% of hydrogen at 160 °C and 100 atm while only 0.8 wt% of hydrogen was recharged into the dehydrogenated pristine sample under the same conditions. Lin et al. [16] have studied the Mg $(NH_2)_2$–$LiNH_2$–4LiH composite in order to improve its kinetics, thermodynamics and cycling properties. While Barison et al. [17] studied the influence of different high energy milling times and of the addition of catalysts such as Nb_2O_5, $TiCl_3$ and graphite on the hydrogen absorption/desorption (A/D) kinetics of a mixture of $2LiNH_2 + 1.1MgH_2$ in the temperature range (220–240) °C. Lan et al. [18] investigated the characteristics of hydrogen storage of $LiNH_2/MgH_2$ (1:1). Albanesi et al. [19] improved the hydrogen sorption kinetics by adding 1 mol% $AlCl_3$ to $LiNH_2$-LiH. They showed that Al^{+3} is incorporated into the $LiNH_2$ structure by partial substitution of Li^+ forming a new amide in the Li–Al–N–H system, which is reversible under hydriding/dehydriding cycles. They assured that the substituted amide improved hydrogen storage properties with respect to $LiNH_2$–LiH. As a result a stable hydrogen storage capacity of about 4.5–5.0 wt% under cycling and completely desorbed in 30 min at 275 °C for the Li–Al–N–H system. Burger et al. [20] studied several material properties, like bulk density and thermodynamic data, isothermal absorption and desorption experiments. They have generated two-step model equations to be utilized to capture the experimentally measured reaction rates and can be used for model validation of the design simulations.

Varin et al. [21] studied the dehydrogenation rate of synthesized hydride nanocomposites of ($LiNH_2 + nMgH_2$). Zhang et al. [22] studied the effect of adding $LiNH_2$ on the hydrogen absorption/desorption capacities of the Li_3N–MgH_2. Albanesi et al. [23] investigated the hydrogen sorption kinetics and the reactions between $LiNH_2$–LiH and $AlCl_3$ additive with a multitechnique approach involving differential scanning calorimetry (DSC), hydrogen volumetric measurements, X-ray powder diffraction (XRPD), Fourier transform infrared analysis (FTIR) and solid-state nuclear magnetic resonance (NMR).

During the current work a special reactor connected to a fully computerized system was designed and fabricated in order to fulfil the needs to study the effect of varying the temperature on the adsorption of hydrogen using Mg–H_2 and $LiNH_2$ at low temperatures (i.e. 25, 30, 35, 40 and 45 °C) based on the gravimetric method. Two mathematical models were generated based on the multiple regression analysis with respect to ANOVA to show the effect of low temperature on hydrogen adsorption for the given candidate materials.

Experimental work

The adsorption of hydrogen using commercial magnesium hydride (i.e. Mg–H_2) supplied by Sigma Aldrich and lithium amide (i.e. $LiNH_2$) supplied by ChemCruz at low temperatures as mentioned previously was investigated using a special hydrogen storage unit which was designed and fabricated in situ. This unit consisted of three major parts, the first part is a

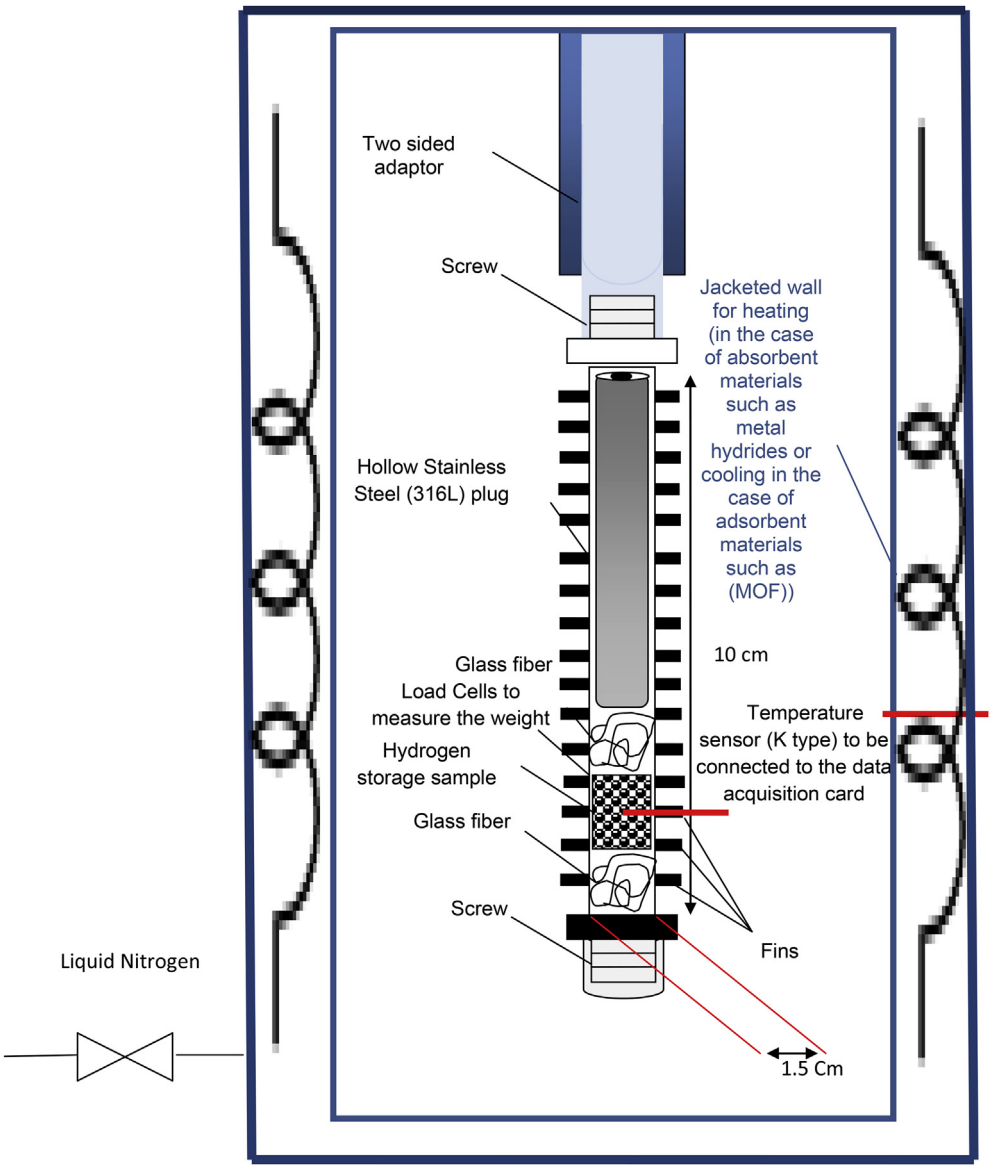

Fig. 1 – A reactor made of stainless steel 316 L used to investigate the adsorption of hydrogen using Mg–H_2 and $LiNH_2$.

reactor made from stainless steel 316 L as shown in Fig. 1, connected to the second part which consisted of piping network made also of stainless steel 316 L, kept inside a glove box as shown in Fig. 2. While the third part is a fully computerized system consisted of measurement and control devices in addition to analogue to digital converters were utilized to build the hydrogen adsorption cycle as shown in Fig. 3.

Before each run, 1 g of Mg–H_2 or $LiNH_2$ weighed using a sensitive balance and kept inside the reactor shown in Fig. 1 before conducting the run, then the reactor was connected to the hydrogen storage unit shown in Fig. 2 followed by flushing the reactor and piping network using inert gas (i.e. He) for three times in order to get rid of oxygen traces. Then hydrogen was introduced to the reactor followed by increasing the reactor temperature to the desired adsorption temperature (i.e. 25, 30, 35, 40 and 45 °C) using certain procedure which included entering the number of hydrogen doses and the time between the doses in order to measure the weight of hydrogen adsorbed within the storage material using the fully computerized system based on the gravimetric method as shown in Fig. 3.

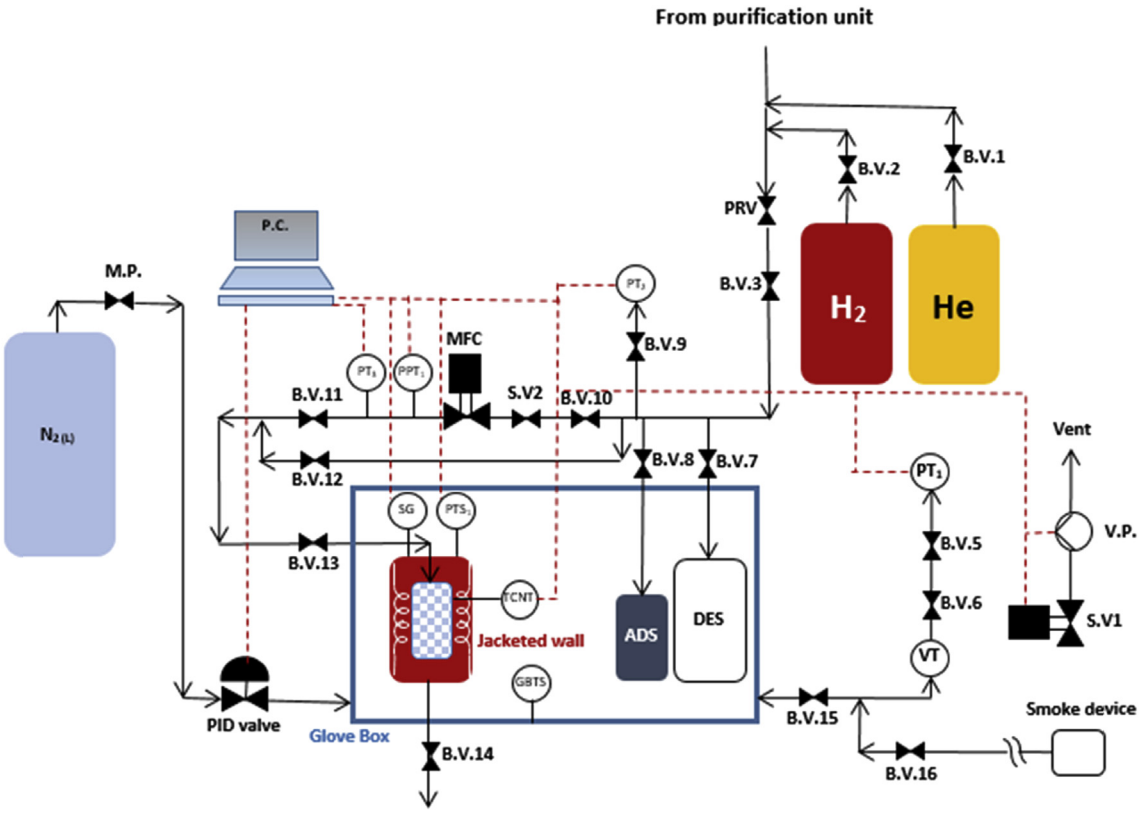

Fig. 2 – Process flow diagram of the hydrogen storage unit.

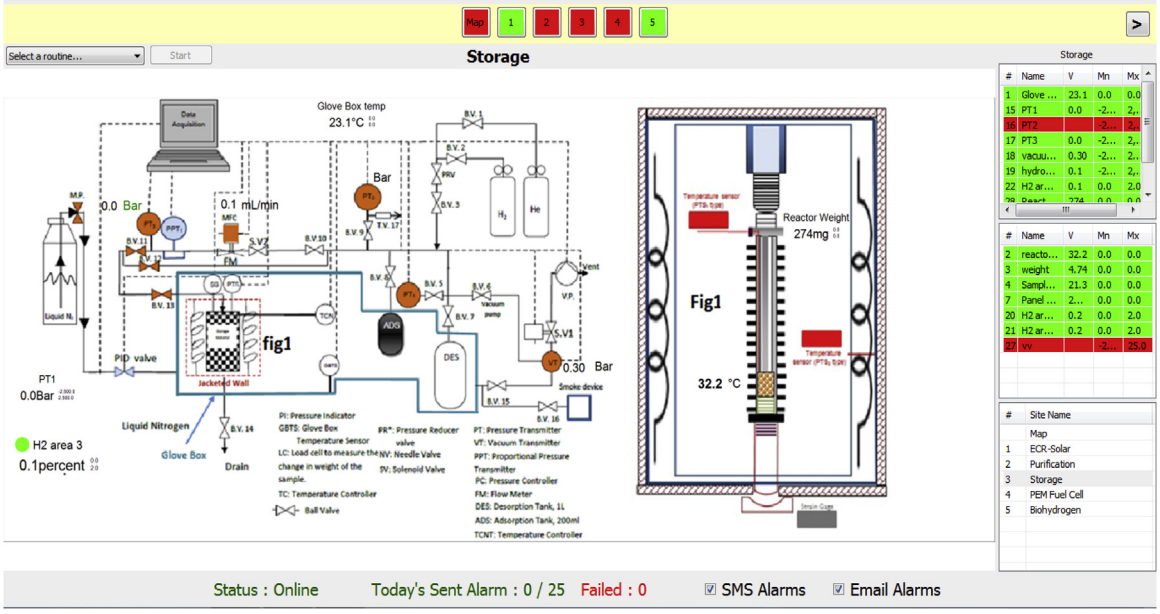

Fig. 3 – Control panel of the software package which was utilized to measure and control the hydrogen adsorption desorption cycles.

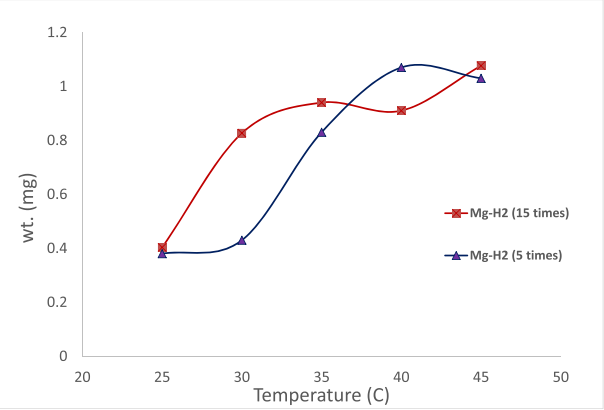

Fig. 4 – Hydrogen adsorption by weight (mg) using two samples of $Mg–H_2$ (i.e. the first sample was used for 15 times while the second sample was used for 5 times).

Results and discussion

Hydrogen storage behaviour of $Mg–H_2$ and $LiNH_2$

Twenty cycles were implemented to measure the adsorption of hydrogen using $Mg–H_2$ at 25, 30, 35, 40 and 45 °C. These cycles were divided into two parts. The first part contained fifteen cycles using the first sample of $Mg–H_2$ (i.e. three cycles per each temperature). Followed by another five cycles using the second sample of $Mg–H_2$ (i.e. one cycle per each temperature) in order to investigate the performance and efficiency of the mentioned material. The results reflected good performance and efficiency which indicates that the candidate material (i.e. $Mg–H_2$) possess long cycle life and cyclibility. Taking into consideration that the obtained results were in agreement with [13,24–29].

On the other hand, ten cycles were implemented to measure the adsorption of hydrogen using $LiNH_2$ at 25, 30, 35, 40 and 45 °C. These cycles were divided into two parts. The first part contained five cycles (i.e. one cycle for each temperature) were implemented using the first sample of $LiNH_2$. Followed by another five cycles (i.e. one cycle for each temperature) using the second sample of $LiNH_2$ in order to investigate the performance and efficiency of the mentioned material in terms of hydrogen storage as shown in Fig. 5. The results were very close to $Mg–H_2$ material which indicates that the candidate material (i.e. $LiNH_2$) possess also long cycle life and cyclibility. All results were in agreement with [13,24–29].

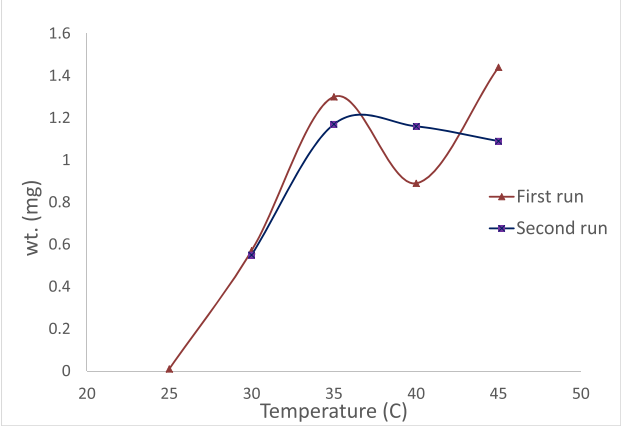

Fig. 5 – Hydrogen adsorption by weight (mg) using two samples of $LiNH_2$ (i.e. the first run represents the first sample while the second run represents the second sample).

Modelling of storage data using $Mg–H_2$ and $LiNH_2$

The models given in Eqs. (1) and (2) were generated after several trials using multiple regression analysis based on the theory of least square error where an optimization was performed by minimizing the error between the predicted values of the response and the actual ones withdrawn from the experimental run. The resulting ANOVA Tables 1–4 for the Eqs. (1) and (2) outline the analysis of variance for the given response (i.e. hydrogen adsorption weight in (mg)) using $Mg–H_2$ in Eq. (1) and $LiNH_2$ in Eq. (2) and the operating condition (i.e. Temperature) as a regressor. Tables 2 and 4 shows also other adequacy measures such as R^2 and Adjusted R^2. The two models assured that the temperature played a vital role in increasing the weight of hydrogen adsorption in both candidate materials (i.e. $Mg–H_2$ and $LiNH_2$) which are in agreement with the results obtained in Figs. 4 and 5. The resulting ANOVA table for both models showed that the adequacy measures R^2 and Adjusted R^2 are close to 1 which are in reasonable agreement and therefore indicate adequate models. An adequate model means that the reduced model has successfully passed all the required statistical tests and can be used to predict the responses [30].It is worth of mention that the entire adequacy measures are in agreement with the general outlines provided by Eltawahni et al. [31] and Eltawahni et al. [32].

For $Mg–H_2$:

$$\text{Wt. (mg)} = -2.06 + 0.133T - 0.00142T^2 \quad (1)$$

where:

Wt.: hydrogen adsorption weight in (mg).
T: Temperature in (°C).

For $LiNH_2$:

$$\text{Wt. (mg)}: -6.316 + 0.3605T - 0.0043T^2 \quad (2)$$

where:

Wt.: hydrogen adsorption weight in (mg).
T: Temperature in (°C).

Table 1 – Analysis of the regressor coefficients given in Eq. (1).

	Coe.	SE	t Stat	P-value
Inter	−2.06	1.09	−1.89	0.1002
T	0.133	0.064	2.08	0.0760
T^2	0.0014	0.0009	−1.56	0.1626

Table 2 – Analysis of variance in addition to R^2 and R^2_{adj}.

ANOVA

	df	SS	MS	F	$F_{critical}$
Reg.	2	0.602	0.3013	20.66	0.001
Res.	7	0.102	0.0146		
Total	9	0.704			
R^2 %	85.5167				
R^2 % (adj.)	81.3786				

Table 3 – Analysis of the regressor coefficients given in Eq. (2).

	Coe.	SE	t Stat	P-value
Inter	−6.316	1.819648	−3.471	0.010392
T	0.3605	0.107074	3.36682	0.011972
T^2	−0.0043	0.001524	−2.82115	0.025731

Table 4 – Analysis of variance in addition to R^2 and R^2_{adj}.

ANOVA

	df	SS	MS	F	$F_{critical}$
Reg.	2	2.0937	1.04685	25.74915	0.000593
Res.	7	0.28459	0.040656		
Total	9	2.37829			
R^2 %	88.03				
R^2 % (adj.)	84.61				

Conclusions

Investigating the hydrogen adsorption at the proposed range of temperatures (25–45° C) using Mg–H_2 and $LiNH_2$ showed that both candidate materials possessed long cycle life and cyclibility which opens the wide door to store hydrogen at ambient conditions which is considered very crucial in hydrogen vehicles powered by PEM fuel cells. On the other hand the generated mathematical models based on the multiple regression analysis with respect to ANOVA revealed that increasing temperature will increase the weight of hydrogen adsorption using Mg–H_2 and $LiNH_2$ respectively.

Acknowledgements

The authors would like to thank the 'Support to Research, Technological Development & Innovation in Jordan' (SRTD – II), an EU funded project managed by the Higher Council for Science & Technology of Jordan for financing the research activities of the current work under the grant no. SRTD/2014/GRT/AR/2321.

REFERENCES

[1] Al-Hadeethi F, Alsyouri H, Al-Ghandoor A, Al-Husban Y, Abdelhadi A, Al-Weissi S. Developing an integrated solar powered system to generate hydrogen from Sea Water. Int J Electrochem Sci 2013;6:6311–20.

[2] Gonzatti F, Farret FA. Mathematical and experimental basis to model energy storage systems composed of electrolyzer, metal hydrides and fuel cells. Energy Convers Manag J 2017;132:241–50.

[3] Wu H, Zhou X, Rodriguez E, Zhou W, Udovic T, Yildirim T, et al. A new family of metal borohydride guanidinate complexes: synthesis, structures and hydrogen-storage properties. J Solid State Chem 2016;242:186–92.

[4] Frya C, Granta D, Walker G. Improved hydrogen cycling kinetics of nano-structured magnesium/transition metal multilayer thin films. Int J Hydrogen Energy 2013;38:982–90.

[5] Shahi R, Tiwari A, Shaz M, Srivastava O. Studies on de/rehydrogenation characteristics of nanocrystalline MgH_2 co-catalyzed with Ti, Fe and Ni. Int J Hydrogen Energy 2013;38:2778–84.

[6] James Jr C, Brinkman K, Gray J, Concepcion J, Anton D. Fundamental environmental reactivity testing and analysis of the hydrogen storage material $2LiBH_4 \cdot MgH_2$. Int J Hydrogen Energy 2014;39:1371–81.

[7] Utke R, Thiangviriya S, Javadian P, Laipple D, Pistidda C, Bergemann N, et al. Effective nanoconfinement of $2LiBH_4$–MgH_2 via simply MgH_2 premilling for reversible hydrogen storages. Int J Hydrogen Energy 2014;39:15614–26.

[8] Mustafa N, Ismail M. Influence of K_2TiF_6 additive on the hydrogen sorption properties of MgH_2. Int J Hydrogen Energy 2014;39:15563–9.

[9] Song M, Kwak Y, Shin H, Lee S, Kim B. Improvement of hydrogen-storage properties of MgH_2 by Ni, $LiBH_4$, and Ti addition. Int J Hydrogen Energy 2013;38:1910–7.

[10] Gattiaa D, Montonea A, Pasquini L. Microstructure and morphology changes in MgH_2/expanded natural graphite pellets upon hydrogen cycling. Int J Hydrogen Energy 2013;38:1918–24.

[11] Korablov D, Ångström J, Ley M, Sahlberg M, Besenbacher F, Jensen T. Activation effects during hydrogen release and uptake of MgH_2. Int J Hydrogen Energy 2014;39:9888–92.

[12] Shao H, Maa W, Kohno M, Takata Y, Xin G, Fujikawa S, et al. Hydrogen storage and thermal conductivity properties of Mg-based materials with different structures. Int J Hydrogen Energy 2014;39:9918–23.

[13] Rusman N, Dahari M. A review on the current progress of metal hydrides material for solid-state hydrogen storage applications. Int J Hydrogen Energy 2016;41:12108–26.

[14] Tran X, McDonald S, Gu Q, Yamamoto T, Shigematsu K, Aso K, et al. In-situ investigation of the hydrogen release mechanism in bulk Mg_2NiH_4. J Power Sources 2017;341:130–8.

[15] Li B, Liu Y, Gu J, Gu Y, Gao M, Pan H. Mechanistic investigations on significantly improved hydrogen storage performance of the $Ca(BH_4)_2$-added $2LiNH_2/MgH_2$ system. Int J Hydrogen Energy 2013;38:5030–8.

[16] Lin H, Li H, Paik B, Wang J, Akiba E. Improvement of hydrogen storage property of three-component $Mg(NH_2)_2$–$LiNH_2$–LiH composites by additives. Dalton Trans 2016;45:15374–81.

[17] Barison S, Agresti F, Lo Russo S, Maddalena A, Palade P, Principi G, et al. A study of the $LiNH_2$–MgH_2 system for solid state hydrogen storage. J Alloys Compd 2008;459:343–7.

[18] Lan Z, Liu S, Li S, Wei W, Guo J. Hydrogen storage properties of $LiNH_2/MgH_2$ complex materials with Ti catalyst by mechanical alloying. Adv Mater Res 2014;898:93–7.

[19] Albanesi L, Larochette P, Gennari F. Destabilization of the $LiNH_2$-LiH hydrogen storage system by aluminum incorporation. Int J Hydrogen Energy 2013;38:12325–34.

[20] Burger I, Hu J, Vitillo J, Kalantzopoulos G, Deledda S, Fichtner M, et al. Material properties and empirical rate

equations for hydrogen sorption reactions in 2 $LiNH_2$–1.1 MgH_2–0.1 $LiBH_4$-3 wt.% $ZrCoH_3$. Int J Hydrogen Energy 2014;39:8238–92.
[21] Varin RA, Parviz R, Polanski M, Wronski Z. The effect of milling energy input and molar ratio on the dehydrogenation and thermal conductivity of the ($LiNH_2$ + $nMgH_2$) [n = 0.5, 0.7, 0.9, 1.0, 1.5 and 2.0] nanocomposites. Int J Hydrogen Energy 2014;39:10585–99.
[22] Zhang B, Wu Y. Storage properties for the Li_3N-MgH_2 system by addition of $LiNH_2$ during the hydrogenation/dehydrogenation. Int J Hydrogen Energy 2015;40:9298–305.
[23] Albanesi L, Garroni S, Larochette P, Nolis P, Mulas G, Enzo S, et al. Role of aluminum chloride on the reversible hydrogen storage properties of the Li-N-H system. Int J Hydrogen Energy 2015;40:13506–17.
[24] Dong B, Gao J, Teng Y, Tian H, Wang L. A novel hydrogen storage system of $KLi_3(NH_2)_4$-4LiH with superior cycling stability. Int J Hydrogen Energy 2016;41:5371–7.
[25] Liu Z, Li Y, Bu Q, Guzy C, Li Q, Chen W, et al. Novel fuel cell stack with coupled metal hydride containers. J Power Sources 2016;328:329–35.
[26] Pottmaier D, Dolci F, Orlova M, Vaughan G, Fichtner M, Lohstroh W, et al. Hydrogen release and structural transformations in $LiNH_2$–MgH_2 systems. J Alloys Compd 2011;5095:5719–23.
[27] Yu X, Yang Z, Guoa Y, Li S. Thermal decomposition performance of $Ca(BH_4)_2$/$LiNH_2$ mixtures. J Alloys Compd 2011;5095:5724–7.
[28] Zhang B, Wu Y. Effects of additives on the microstructure and hydrogen storage properties of the Li_3N–MgH_2 mixture. J Alloys Compd 2014;613:199–203.
[29] Dong B, Wang L, Teng Y, Li Z, Zhao J. Superior effect of RbF on decreasing the dehydrogenation operating temperature of the $LiNH_2$-LiH system. J Alloys Compd 2017;613:62–7.
[30] Ekpeni L, Benyounis K, Stokes J, Olabi Abdul G. Improving and optimizing protein concentration yield from homogenized baker's yeast at different ratios of buffer solution. Int J Hydrogen Energy 2016;41:16415–27.
[31] Eltawahni H, Hagino M, Benyounis K, Inoue T, Olabi AG. Effect of CO_2 laser cutting process parameters on edge quality and operating cost of AISI316L. Opt Laser Technol J 2012;44:1068–82.
[32] Eltawahni H, Olabi A, Benyounis K. Effect of process parameters and optimization of CO_2 laser cutting of ultra high-performance polyethylene. Mater Des J 2010;31:4029–38.

Nomenclature

ANOVA: analysis of variance
MOFs: metal organic frameworks
TEM: transmission electron microscopy
XRPD: X-ray powder diffraction
DSC: differential scanning calorimetry
PI: pressure indicator
GBTS: glove box temperature sensor for hydrogen
LC: load cell to measure the change in weight of the sample
TC: temperature controller
DES: desorption tank
ADS: adsorption tank
PC: pressure controller
TCNT: temperature controller
NV: needle valve
SV: solenoid valve
PT: pressure transmitter
VT: vacuum transmitter
PRT: proportional pressure transmitter
FM: flow meter
FTIR: Fourier transform infrared
NMR: nuclear magnetic resonance
Wt.: weight
T: temperature
R^2: regression factor
Coe: coefficient
SE: standard deviation
t Stat: t-test
P: P-value
df: degrees of freedom
SS: sum of squares
MS: mean square
F: F-value